2-4-2005

Ligand Rotation in $[Ar(R)N]_3M\text{-}N_2\text{-}M'[N(R)Ar]_3$ (M, M' = Mo^{III}, Nb^{III}; R = ^{i}Pr and ^{t}Bu) Dimers

Gemma J. Christian
Avondale College, gemma.christian@avondale.edu.au

Robert Stranger
Australian National University

Brian F. Yates
University of Tasmania

David C. Graham
University of Tasmania

Recommended Citation

Christian, G., Stranger, R., Yates, B. F., & Graham, D. C. (2005). Ligand rotation in $[Ar(R)N]_3M\text{-}N_2\text{-}M'[N(R)Ar]_3$ (M, M' = Mo^{III}, Nb^{III}; R = ^{i}Pr and ^{t}Bu) dimers. *Dalton Transactions*, 2005(5), 962–968. doi:10.1039/B413766C

FULL PAPER

Dalton
www.rsc.org/dalton

Ligand rotation in $[Ar(R)N]_3M\text{-}N_2\text{-}M'[N(R)Ar]_3$ (M, M′ = Mo^{III}, Nb^{III}; R = ^{i}Pr and ^{t}Bu) dimers

Gemma Christian,[a] Robert Stranger,*[a] Brian F. Yates[b] and David C. Graham[b]

[a] *Department of Chemistry, Faculty of Science, Australian National University, Canberra, ACT 0200, Australia*

[b] *School of Chemistry, University of Tasmania, Private Bag 75, Hobart, TAS 7001, Australia*

Received 7th September 2004, Accepted 18th January 2005
First published as an Advance Article on the web 4th February 2005

Earlier calculations on the model N_2-bridged dimer $(\mu\text{-}N_2)\text{-}\{Mo[NH_2]_3\}_2$ revealed that ligand rotation away from a trigonal arrangement around the metal centres was energetically favourable resulting in a reversal of the singlet and triplet energies such that the singlet state was stabilized 13 kJ mol^{-1} below the D_{3d} triplet structure. These calculations, however, ignored the steric bulk of the amide ligands N(R)Ar (R = ^{i}Pr and ^{t}Bu, Ar = 3,5-$C_6H_3Me_2$) which may prevent or limit the extent of ligand rotation. In order to investigate the consequences of steric crowding, density functional calculations using QM/MM techniques have been performed on the $Mo^{III}Mo^{III}$ and $Mo^{III}Nb^{III}$ intermediate dimer complexes $(\mu\text{-}N_2)\text{-}\{Mo[N(R)Ar]_3\}_2$ and $[Ar(R)N]_3Mo\text{-}(\mu\text{-}N_2)\text{-}Nb[N(R)Ar]_3$ formed when three-coordinate $Mo[N(R)Ar]_3$ and $Nb[N(R)Ar]_3$ react with dinitrogen. The calculations indicate that ligand rotation away from a trigonal arrangement is energetically favourable for all of the ligands investigated and that the distortion is largely electronic in origin. However, the steric constraints of the bulky amide groups do play a role in determining the final orientation of the ligands, in particular, whether the ligands are rotated at one or both metal centres of the dimer. Analogous to the model system, QM/MM calculations predict a singlet ground state for the $(\mu\text{-}N_2)\text{-}\{Mo[N(R)Ar]_3\}_2$ dimers, a result which is seemingly at odds with the experimental triplet ground state found for the related $(\mu\text{-}N_2)\text{-}\{Mo[N(^{t}Bu)Ph]_3\}_2$ system. However, QM/MM calculations on the $(\mu\text{-}N_2)\text{-}\{Mo[N(^{t}Bu)Ph]_3\}_2$ dimer reveal that the singlet–triplet gap is nearly 20 kJ mol^{-1} smaller and therefore this complex is expected to exhibit very different magnetic behaviour to the $(\mu\text{-}N_2)\text{-}\{Mo[N(R)Ar]_3\}_2$ system.

1 Introduction

The abundant and ready supply of molecular nitrogen makes it very appealing as a potential feedstock in industrial processes used to generate nitrogen-containing compounds. However, the extremely high kinetic barrier to cleaving the strong N≡N triple bond presents a significant chemical challenge to finding systems that can activate dinitrogen under relatively mild conditions.[1,2] Towards this goal, a recent discovery of interest is the reaction involving the coordinatively unsaturated, Mo(III) complex developed by Laplaza and Cummins.[3] In this reaction, the sterically hindered, three-coordinate complex $Mo[N(R)Ar]_3$ (R = $C(CH_3)_3$, Ar = 3,5-$C_6H_3Me_2$) spontaneously reacts with dinitrogen resulting in its cleavage, *via* a N_2-bridged dimeric intermediate, to form the nitrido product $[Ar(R)N]_3MoN$.

The cleavage of N_2 by $Mo[N(R)Ar]_3$ complexes has been the focus of several computational studies.[4–8] On the basis of a DFT (density functional theory) study using a smaller model system, $Mo[NH_2]_3$, Morokuma *et al.*[4] suggested that the first step in the above reaction is the coordination of N_2 to $Mo[NH_2]_3$ to form the $N_2\text{-}Mo[NH_2]_3$ encounter complex as shown in Fig. 1. This is followed by coordination of a second $Mo[NH_2]_3$ complex to form the intermediate $(\mu\text{-}N_2)\text{-}\{Mo[NH_2]_3\}_2$ dimer with a triplet ground state. The system then undergoes spin crossover to the spin singlet state which lies slightly higher in energy. Cleavage of dinitrogen occurs *via* a singlet transition state with a significantly elongated N–N bond to form the $[NH_2]_3MN$ product also in the singlet spin state. The thermodynamic driving force for the cleavage reaction is the formation of the strong Mo≡N bonds.

The intermediate dimer, $(\mu\text{-}N_2)\text{-}\{Mo[N(R)Ar]_3\}_2$ has been isolated experimentally and structurally characterized.[9] EXAFS data and Raman spectra indicate an approximately linear Mo–N–N–Mo core with a N–N bond length of 1.19 Å or 1.23 Å, respectively. SQUID magnetometry studies on the related $(\mu\text{-}N_2)\text{-}\{Mo[N(^{t}Bu)Ph]_3\}_2$ dimer give a magnetic moment of μ = 2.85 μ_B consistent with the spin triplet ground state predicted from Morokuma's calculations.

In our recent DFT study[6] involving the reaction of dinitrogen with the model complex $Mo[NH_2]_3$, we calculated a triplet ground state for the intermediate dimer if the NH_2 ligands maintained trigonal symmetry around the metal centres corresponding to the D_{3d} dimer structure shown in Fig. 2. The triplet structure is consistent with those reported by other workers using DFT methods.[4,5] However, unexpectedly, our calculations revealed that a lower energy C_{2h} dimer structure existed where one ligand at each metal centre is rotated around the Mo–N_L

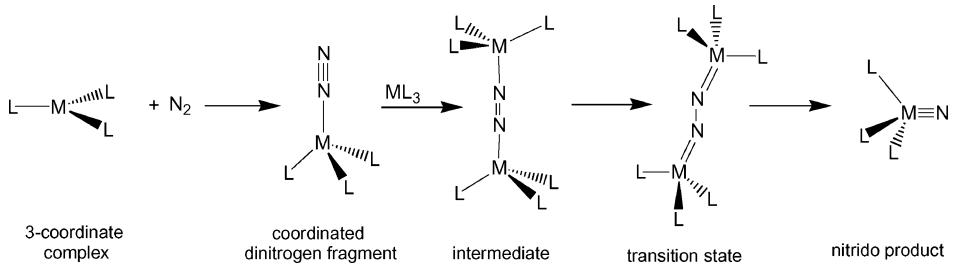

Fig. 1 Reaction mechanism for N_2 cleavage by MoL_3, L = NH_2.

DOI: 10.1039/b413766c

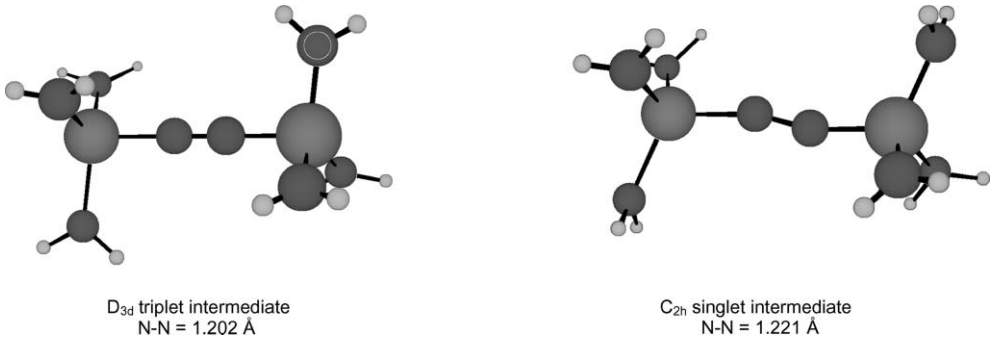

Fig. 2 Ligand rotation in the model $Mo^{III}Mo^{III}$ intermediate dimer $(\mu\text{-}N_2)\text{-}\{Mo[NH_2]_3\}_2$.

axis by 90° as seen in Fig. 2. The ligand rotation optimises the π donation from the NH_2 groups to the metal, which in turn enhances the π-back donation from the metal to the dinitrogen fragment, consequently increasing the level of N_2 activation. The distortion results in a further stabilization of the singlet spin state by 56 kJ mol^{-1} bringing it below the triplet state by 13 kJ mol^{-1} in energy. Our calculations on the model system therefore predict a C_{2h} spin singlet ground state structure for the intermediate dimer which is seemingly at odds with the reported triplet ground state observed for the related $(\mu\text{-}N_2)\text{-}\{Mo[N(^tBu)Ph]_3\}_2$ system.

Intuitively, rotation of the ligands in the experimental system seems unlikely because of their bulky size. However, ligand rotation is observed in the crystal structure of the related $Mo^{III}Nb^{III}$ dimer $[Ar(^tBu)N]_3Mo\text{-}(\mu\text{-}N_2)\text{-}Nb[N(^iPr)Ar]_3$ (Ar = 3,5-$C_6H_3Me_2$).[10] This dimer possesses a significantly activated dinitrogen bridge (N–N bond length of 1.235 Å) and when KC_8 is used as a reducing agent, results in cleavage of the N–N bond. Our recent calculations on the model complex $(H_2N)_3Mo\text{-}(\mu\text{-}N_2)\text{-}Nb(NH_2)_3$ agree with the experimental findings and show that although the N_2 bridge is significantly activated, cleavage of the N–N bond does not occur due to a sizeable endothermic cleavage step calculated at 144 kJ mol^{-1}.[8] The reluctance of the dimer to cleave the N–N bond was shown to be a consequence of the d^3d^2 $Mo^{III}Nb^{III}$ metal configuration which is one electron short of the d^3d^3 configuration necessary to undergo reductive cleavage of the dinitrogen bridge. This was confirmed by additional calculations on the related d^3d^3 systems $[(H_2N)_3Mo^{III}\text{-}(\mu\text{-}N_2)\text{-}Nb^{II}(NH_2)_3]^{1-}$ and $[(H_2N)_3Nb^{II}\text{-}(\mu\text{-}N_2)\text{-}Nb^{II}(NH_2)_3]^{2-}$ which were shown to have substantially exothermic N_2 cleavage steps.

Interestingly, although the crystal structure of $[Ar(^tBu)N]_3\text{-}Mo\text{-}(\mu\text{-}N_2)\text{-}Nb[N(^iPr)Ar]_3$ does exhibit ligand rotation, it only occurs for the $N(^iPr)Ar$ ligands bound to Nb and not the $N(^tBu)Ar$ groups coordinated to Mo. Even though the $N(^iPr)Ar$ group is smaller in size than $N(^tBu)Ar$, the structure of this complex demonstrates that rotation of the bulky ligands is possible in these systems. This observation raises several questions. Is the ligand orientation observed in the $Mo^{III}Nb^{III}$ dimer due to the smaller size of the $N(^iPr)Ar$ groups relative to $N(^tBu)Ar$, or the result of a greater electronic driving force for rotation because two different metal ions are involved? Since ligand rotation is possible, does it occur in the $(\mu\text{-}N_2)\text{-}\{Mo[N(R)Ar]_3\}_2$ dimer for R = ^{i}Pr or R = ^{t}Bu and if so, what effect does this have on the ground state of the dimer given that calculations on the model system indicate a significant stabilization of the singlet state over the triplet when ligand rotation is allowed?

The cleavage of N_2 by the three-coordinate complex $Mo[N(^iPr)Ar]_3$ has also been studied experimentally but the $(\mu\text{-}N_2)\text{-}\{Mo[N(^iPr)Ar]_3\}_2$ dimer intermediate has not been observed, presumably due to even more facile cleavage of N_2 as a result of the smaller size of the $N(^iPr)Ar$ ligand.[11] In the absence of crystal data for the $(\mu\text{-}N_2)\text{-}\{Mo[N(R)Ar]_3\}_2$ dimer, the problem lends itself to a theoretical study involving combined DFT and MM calculations where the steric bulk of the ligands can be incorporated through MM while DFT is applied to the electronically important regions.

The purpose of this study is to investigate the energetic and structural effects of ligand rotation in both $L_3Mo^{III}\text{-}(\mu\text{-}N_2)\text{-}Mo^{III}L_3$ and $L_3Mo^{III}\text{-}(\mu\text{-}N_2)\text{-}Nb^{III}L_3$ dimers using DFT methods. Calculations are carried out first on the model systems, where L = NH_2, in order to compare the effect of ligand rotation for the two dimers in the absence of steric strain. The effect of the size of the bulky substituents on the ligand orientation is then examined through QM/MM calculations on the experimental systems with L = N(R)Ar (R = ^{i}Pr, ^{t}Bu; Ar = 3,5-$C_6H_3Me_2$).

2 Computational details

The calculations carried out in this work were performed using the Amsterdam Density Functional (ADF)[12–14] program (version 2002.03) running on either Linux-based Pentium IV computers or the Australian National University Supercomputing Facility. All calculations used the local density approximation (LDA) to the exchange potential, the correlation potential of Vosko, Wilk and Nusair (VWN),[15] the Becke[16] and Perdew[17] corrections for non-local exchange and correlation, and the numerical integration scheme of te Velde and co-workers.[18] Geometry optimisations were performed using the gradient algorithm of Versluis and Ziegler.[19] All electron, triple-ζ Slater type orbital basis sets (TZP) were used for all atoms. Relativistic effects were incorporated using the zero order relativistic approximation (ZORA)[20–22] functionality in ADF. Frequencies were computed in ADF by numerical differentiation of energy gradients in slightly displaced geometries.[23,24] All calculations were carried out in a spin-unrestricted manner, and for the model systems were performed in either D_{3d}, C_{2h}, or C_s symmetry for the $Mo^{III}Mo^{III}$ dimer and C_{3v} or C_s symmetry for the $Mo^{III}Nb^{III}$ dimer, depending on the number of ligands rotated on each metal centre and whether ligands were rotated at only one or both metal centres. Frequency calculations were used to confirm that the optimized structures of lowest energy were true minima.

For the experimental $M[N(R)Ar]_3$ and $M[N(R)Ph]_3$ systems the QM/MM[25] method implemented in ADF was used. For these calculations, the system under study is partitioned into two regions one of which is treated with DFT and the other with force field methods. Typically, the electronically important parts of the molecule are included in the QM region. Accordingly, N_2, the N donors from the amide ligands, Mo and Nb, were treated with DFT while the ^{i}Pr, ^{t}Bu, 3,5-$C_6H_3Me_2$ and C_6H_5 substituents were treated with molecular mechanics using the Sybyl[26] force field available in ADF. UFF van der Waals parameters[27] were used for Mo and Nb atoms and all other parameters involving the metal atoms were set to zero. The bonds that cross the QM/MM partition, known as link bonds, were "capped" by H for the QM region. The ratio of the link bond to the length of the capping bond was kept constant throughout the calculations corresponding to the link bond parameters being fixed at values of $a_{(N-C(R))}$ = 1.489 and $a_{(N-C(Ar))}$ = 1.412. This partitioning

scheme is very similar to that used in the study of N_2O cleavage by $Mo[N(R)Ar]_3$.[28] All QM/MM calculations on the experimental systems were undertaken in C_1 symmetry although constraints were used in some cases to impose local C_3 symmetry around each metal.

3 Results and discussion

3.1 Model system, L = NH_2

DFT calculations were carried out on the model systems used in previous studies,[4–6] where the bulky N(R)Ar groups are replaced with simple NH_2 ligands. The effect of ligand rotation on the energy of the complexes was examined for both the $(H_2N)_3Mo$-(μ-N_2)-$Mo(NH_2)_3$ and $(H_2N)_3Mo$-(μ-N_2)-$Nb(NH_2)_3$ dimers. Several ligand orientations were explored, shown in Fig. 3. These included a trigonal arrangement (no ligand rotation, **a**, linear, and **b**, bent, in Fig. 3), a structure with one ligand rotated by 90° at a single metal center and one with a ligand rotated at both metal centers (**c** and **d** in Fig. 3). The results of the calculations are summarized in Table 1 for both

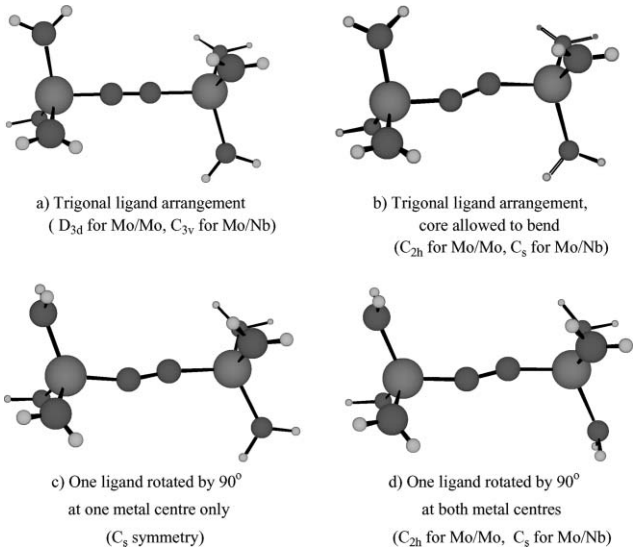

Fig. 3 Different ligand orientations for the model $Mo^{III}Mo^{III}$ and $Mo^{III}Nb^{III}$ intermediate dimers (μ-N_2)-{$Mo[NH_2]_3$}$_2$ and $(H_2N)_3Mo$-(μ-N_2)-$Nb(NH_2)_3$.

the $Mo^{III}Mo^{III}$ and $Mo^{III}Nb^{III}$ systems. Additional calculations in C_1 symmetry did not reveal any lower energy structures.

The ground state structure of the $Mo^{III}Nb^{III}$ dimer was calculated to be a spin doublet, in agreement with experiment, and possesses C_s symmetry with one ligand rotated at both metal centres. The experimental structure on the other hand, only exhibits ligand rotation at the Nb centre. The lowest lying spin quartet structure also has C_s symmetry with one ligand rotated at each metal centre, but is calculated to lie 132 kJ mol^{-1} higher in energy. The calculated N–N bond length of 1.237 Å for the $Mo^{III}Nb^{III}$ dimer is in close agreement with the experimentally observed bond length of 1.235 Å.[10] Despite the long N–N bond, cleavage of the coordinated N_2 is unfavourable with the products, $NMo[NH_2]_3$ and $NNb[NH_2]_3$, destabilized relative to the intermediate dimer by 144 kJ mol^{-1}.[8]

As already mentioned, the $Mo^{III}Mo^{III}$ dimer has a triplet ground state when a trigonal arrangement of the ligands is maintained around the metal centres but the singlet state is stabilized below the triplet if one ligand on each metal centre is allowed to rotate by approximately 90° to give a C_{2h} dimer structure (Fig. 3, structure **d**). Unlike the large spin doublet–quartet gap calculated for the $Mo^{III}Nb^{III}$ dimer, the corresponding spin singlet–triplet gap for the $Mo^{III}Mo^{III}$ dimer is considerably smaller, with the triplet state calculated to lie only 13 kJ mol^{-1} higher in energy than the singlet.

For both $Mo^{III}Mo^{III}$ and $Mo^{III}Nb^{III}$ systems, ligand rotation at one or both metal centres results in additional stabilization of the dimer relative to the structures having a trigonal arrangement of the ligands. Unfortunately, the trigonal (D_{3d}) singlet structure cannot be represented by a single determinant configuration and therefore it was necessary to use spin projection in order to obtain its energy.[29,30] The advantage gained by rotating one ligand at both metal centres is about 47 kJ mol^{-1} for the $Mo^{III}Nb^{III}$ dimer and 56 kJ mol^{-1} for the $Mo^{III}Mo^{III}$ dimer in the doublet and singlet spin states, respectively. With the exception of the $Mo^{III}Mo^{III}$ dimer in the triplet state, the greatest stabilization occurs when the ligands are rotated at both metal centres. However, it is worth noting that for the $Mo^{III}Nb^{III}$ dimer in the doublet spin state, the stabilization gained by rotating just one ligand at the Nb centre is 37 kJ mol^{-1}, only 10 kJ mol^{-1} less than the stabilization gained by rotating two ligands. For the $Mo^{III}Mo^{III}$ dimer, the gain is 37 kJ mol^{-1} for rotation at one centre for the singlet, compared to 56 kJ mol^{-1} for both. Clearly, the driving force for ligand rotation is affected by the identity of the metal centres.

Table 1 The effect of ligand (NH_2) rotation on the energy of the $Mo^{III}Mo^{III}$ and $Mo^{III}Nb^{III}$ model dimers

Dimer (spin state)	Symmetry	Ligand rotation[a]	ΔE^b/kJ mol^{-1}	ΔE^c/kJ mol^{-1}	N–N/Å
$Mo^{III}Mo^{III}$ ($S = 0$)	D_{3d}	Trigonal[d,e]	−185.35		
	C_{2h}	None	−202.29	−16.95	1.202
	Cs	One metal only	−222.63	−37.28	1.215
	C_{2h}	Both metals	−241.01	−55.66	1.221
$Mo^{III}Mo^{III}$ ($S = 1$)	D_{3d}	Trigonal	−224.53		1.202
	C_{2h}	None	−222.38	2.16	1.201
	Cs	One metal only	−229.31	−4.78	1.205
	C_{2h}	Both metals	−228.08	−3.55	1.209
$Mo^{III}Nb^{III}$ ($S = 1/2$)	C_{3v}	Trigonal	−256.17		1.226
	C_s	None[f]	−286.79	−30.62	1.217
	C_s	Mo only	−287.58	−31.42	1.248
	C_s	Nb only	−293.01	−36.85	1.221
	C_s	Both metals	−303.27	−47.10	1.237
$Mo^{III}Nb^{III}$ ($S = 3/2$)	C_{3v}	Trigonal	−106.07		1.185
	C_s	Trigonal	−114.01	−7.94	1.205
	C_s	Mo only	−146.32	−40.25	1.210
	C_s	Nb only	−151.75	−45.68	1.207
	C_s	Both metals	−171.76	−65.69	1.208

[a] Ligand rotation refers to the metal center where the rotation, if any, occurs. In all cases ligand rotation is approximately 90°. [b] Energy relative to reactants. [c] Energy relative to trigonal dimer structure. [d] Not single determinant. Spin projection used to obtain energy.[29,30] [e] Several imaginary frequencies. [f] Ligands on Nb rotate.

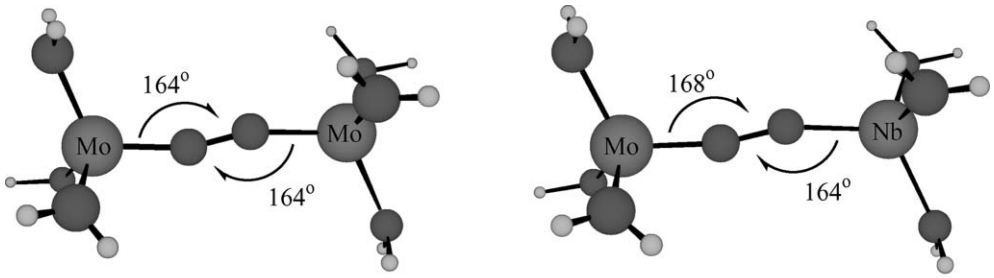

a) Mo/Mo dimer (S=0) Ligands rotated at both metal centres.

b) Mo/Nb dimer (S=1/2) Ligand rotated at both metal centres.

Fig. 4 Optimised structures with bent M–N–N–M cores for the model $Mo^{III}Mo^{III}$ and $Mo^{III}Nb^{III}$ intermediate dimers (μ-N_2)-{Mo[NH_2]$_3$}$_2$ and (H_2N)$_3$Mo-(μ-N_2)-Nb(NH_2)$_3$.

For the $Mo^{III}Nb^{III}$ dimer with C_s symmetry (Fig. 3, structure **b**) there is significant twisting of the ligands away from a trigonal arrangement. Most of the stabilization of the C_s structure relative to C_{3v}, is due to this ligand movement. For the $Mo^{III}Nb^{III}$ and $Mo^{III}Mo^{III}$ structures with ligands rotated at both metal centres, marked bending of the M–N–N–M core occurs as depicted in Fig. 4. Our earlier work has shown that this bending enhances the π overlap between the metal and the coordinated N_2.[6]

In summary, based on the above calculations on the model systems, ligand rotation is favourable for both the $Mo^{III}Nb^{III}$ and $Mo^{III}Mo^{III}$ dimers. In the case of the $Mo^{III}Nb^{III}$ dimer, the structure with a ligand rotated at both metal centres is 10 kJ mol^{-1} more stable than the structure with a ligand rotated at the Nb centre only, the latter corresponding to the ligand arrangement observed in the experimental structure.

From Table 1, it is apparent that the stabilization gained from ligand rotation is actually greater for the $Mo^{III}Mo^{III}$ dimer than for the $Mo^{III}Nb^{III}$ dimer. Thus, given that ligand rotation is observed experimentally for the $Mo^{III}Nb^{III}$ dimer, one might also expect it to be present in the corresponding $Mo^{III}Mo^{III}$ dimer, assuming that the steric constraints in both systems are comparable.

3.2 QM/MM system, L = N(R)Ar

3.2.1 R = ^{i}Pr and R = ^{t}Bu. The effect of the bulky alkyl and aryl groups on the structure and energy of the $Mo^{III}Nb^{III}$ and $Mo^{III}Mo^{III}$ dimers was investigated for the N(^{i}Pr)Ar and N(^{t}Bu)Ar ligands present in the experimental systems using QM/MM methods. In these calculations, the ligands at both the Mo and Nb centres were identical, either N(^{i}Pr)Ar or N(^{t}Bu)Ar, and therefore differed from the real experimental $Mo^{III}Nb^{III}$ system which has N(^{i}Pr)Ar and N(^{t}Bu)Ar ligands at the Nb and Mo centres, respectively. Analogous to the calculations on the model systems, different ligand orientations were investigated including structures where the ligands maintained an approximately trigonal orientation at the metal centers, and structures with a single ligand rotated by 90° at one or both metal centers. The calculated energies of the different structures relative to the reactants are summarized in Table 2.

The results in Table 2 follow similar patterns to the calculated energies for the model systems. For both R = ^{i}Pr and ^{t}Bu, rotation of a single ligand at just one metal centre results in significant stabilization for both the $Mo^{III}Nb^{III}$ and $Mo^{III}Mo^{III}$ dimers, with the structure involving ligand rotation at both metal centres being lowest in energy. Surprisingly, the stabilization due to ligand rotation is greater for the N(^{i}Pr)Ar ligands than for the model systems for both $Mo^{III}Nb^{III}$ and $Mo^{III}Mo^{III}$ dimers. The ability of the ligands to rotate quite freely is demonstrated by the fact that constraints were required to maintain a trigonal arrangement of the ligands around the metal centres for the $Mo^{III}Nb^{III}$ dimer. In the case of the $Mo^{III}Mo^{III}$ dimer, it was not even possible to find a minimum energy structure where the ligands were not rotated.

As found for the model system, ligand rotation for the $Mo^{III}Mo^{III}$ dimer results in significant stabilization of the singlet

Table 2 The effect of ligand rotation on the energy of the $Mo^{III}Mo^{III}$ and $Mo^{III}Nb^{III}$ dimers, with N(R)Ar ligands

Dimer (spin state)	Symmetry	Ligand rotation[a]	ΔE^b/kJ mol^{-1}	ΔE^c/kJ mol^{-1}	N–N/Å
$Mo^{III}Mo^{III}$ R = ^{i}Pr ($S = 0$)	≈C_3	None			
	None	One only	−245.28		1.224
	None	Both	−278.97		1.225
$Mo^{III}Mo^{III}$ R = ^{i}Pr ($S = 1$)	≈C_3	Neither	−230.29		1.206
	None	One only	−235.35	−5.06	1.213
	None	Both	−243.53	−13.24	1.216
$Mo^{III}Mo^{III}$ R = ^{t}Bu ($S = 0$)	≈C_3	None			
	None	One only	−206.34		1.225
	None	Both	−237.55		1.232
$Mo^{III}Mo^{III}$ R = ^{t}Bu ($S = 1$)	≈C_3	None	−196.59		1.214
	None	One only	−196.91	−0.32	1.223
	None	Both	−212.49	−15.90	1.240
$Mo^{III}Nb^{III}$ R = ^{i}Pr ($S = 1/2$)	≈C_3	Trigonal	−280.50		1.225
	None	Mo only[d]	−328.43	−47.94	1.262
	None	Nb only[d]	−329.43	−48.94	1.227
	None	Both metals	−345.71	−65.21	1.241
$Mo^{III}Nb^{III}$ R = ^{t}Bu ($S = 1/2$)	≈C_3	Trigonal	−287.54		1.237
	None	Mo only	−296.69	−9.15	1.212
	None	Nb only	−305.10	−17.56	1.232
	None	Both rotated	−305.11	−17.57	1.209

[a] Ligand rotation refers to the metal center where the rotation, if any, occurs. [b] Energy relative to reactants. [c] Energy relative to ≈C_3 dimer structure. [d] Structure not C_3 at either metal center.

spin state over the triplet such that it becomes the ground state for both R = ^{i}Pr and R = ^{t}Bu. The singlet–triplet separation for R = ^{t}Bu (25 kJ mol^{-1}) is less than that for R = ^{i}Pr (35 kJ mol^{-1}) but greater than the singlet–triplet gap of 13 kJ mol^{-1} for the model system. Optimisation of the approximately trigonal $Mo^{III}Mo^{III}$ dimer in the singlet spin state was problematic. This is not surprising since both the model D_{3d} and real (trigonal) singlet structures cannot be represented by single determinant wavefunctions. However, once the trigonal symmetry is broken, for example by allowing ligand rotation, the problem is removed. The stabilization due to ligand rotation is at least 34 kJ mol^{-1} for R = ^{i}Pr and 31 kJ mol^{-1} for R = ^{t}Bu (relative to the structures involving rotation at one metal centre) but without the energy of the trigonal structure it is not feasible to determine the stabilization more precisely. Furthermore, since there is no crystal data for either the (μ-N_2)-{Mo[N(^{t}Bu)Ar]$_3$}$_2$ or (μ-N_2)-{Mo[N(^{t}Bu)Ph]$_3$}$_2$ dimers, it is not possible to compare our calculated structures with experiment. Suffice to say that the calculated N–N bond distances of 1.232 and 1.225 Å for R = ^{t}Bu and R = ^{i}Pr, respectively, are within the range of distances determined from EXAFS and Raman measurements on (μ-N_2)-{Mo[N(^{t}Bu)Ar]$_3$}$_2$.

For the $Mo^{III}Nb^{III}$ dimer, the stabilization due to ligand rotation is significantly less for the N(^{t}Bu)Ar ligand compared to N(^{i}Pr)Ar, indicating that the size of the bulky substituents does influence the overall energetics. For the spin doublet, the rotated structure is stabilized by 18 kJ mol^{-1} when R = ^{t}Bu compared to 65 kJ mol^{-1} for R = ^{i}Pr and 47 kJ mol^{-1} for the model system. In fact, for R = ^{t}Bu, the structure with ligands rotated at both metal centres and the structure where a ligand is rotated only at Nb are equivalent in energy. The analogous structure where the ligand rotation is only at the Mo centre is 8 kJ mol^{-1} less stable. In contrast, for R = ^{i}Pr, the structures with one ligand rotated at either the Mo or Nb centres differ by only 1 kJ mol^{-1}. The calculated N–N bond distances of 1.232 and 1.241 Å for R = ^{t}Bu and R = ^{i}Pr, respectively, are very close to the experimentally observed distance of 1.235 Å for the [Ar(^{t}Bu)N]$_3$Mo-(μ-N_2)-Nb[N(^{i}Pr)Ar]$_3$ complex.

The lowest energy optimised structures for the $Mo^{III}Mo^{III}$ dimer with L = N(^{i}Pr)Ar and N(^{t}Bu)Ar are shown in Fig. 5. The corresponding $Mo^{III}Nb^{III}$ dimers have similar structures. For both systems, one amide ligand at each metal centre is rotated so that it is perpendicular to the M–N–N–M plane. Stacking of the phenyl rings is also evident in the rotated structures of both the $Mo^{III}Mo^{III}$ and $Mo^{III}Nb^{III}$ dimers for R = ^{i}Pr and R = ^{t}Bu and appears to be present in the crystal structure of the experimental system.[10] The M–N–N–M core of the dimers seems to be quite free to bend when R = ^{i}Pr, despite the steric bulk. For example, in the case of the $Mo^{III}Nb^{III}$ dimer with ligands rotated at both metal centres, the Mo–N–N angle of 166° is very similar to the angle of 168° found for the model system. However, for R = ^{t}Bu, the increased steric crowding restricts the bending of the Mo–N–N–Mo core such that the Mo–N–N angle is now 175°. Perhaps more importantly, the size of the R group also influences the N–N bond lengths which tend to be slightly longer for R = ^{t}Bu than R = ^{i}Pr, and in both cases are longer than those calculated for the model system.

Our calculations indicate that while the steric bulk of the ligands does influence the overall structures and energetics of these dimers, ligand rotation should still be favourable for the $Mo^{III}Mo^{III}$ dimer and consequently, a singlet ground state is predicted, at odds with the triplet ground state observed for the related (μ-N_2)-{Mo[N(^{t}Bu)Ph]$_3$}$_2$ system. For the $Mo^{III}Nb^{III}$ dimer, a rotated ligand structure is also favourable but the size of the R group has a greater influence on the orientation of the ligands in the intermediate dimer and whether or not rotation occurs at one or both metal centres.

3.2.2 Experimental $Mo^{III}Nb^{III}$ system. In the experimental system, [Ar(^{t}Bu)N]$_3$Mo-(μ-N_2)-Nb[N(^{i}Pr)Ar]$_3$, both R = ^{t}Bu and R = ^{i}Pr groups are present and the reported crystal structure reveals that ligand rotation only occurs at the Nb centre. Unfortunately, the above calculations on the $Mo^{III}Nb^{III}$ system have not provided an unambiguous result regarding ligand orientation since ligand rotation at both Mo and Nb centres was predicted for R = ^{i}Pr whereas when R = ^{t}Bu, the structure involving ligand rotation at both metal centres and the structure with ligand rotation at Nb only, were equivalent in energy. Thus, it was necessary to make a direct comparison with experiment and undertake QM/MM calculations on the mixed metal and mixed ligand system [Ar(^{t}Bu)N]$_3$Mo-(μ-N_2)-Nb[N(^{i}Pr)Ar]$_3$. The results of the calculations on the experimental system are shown in Table 3.

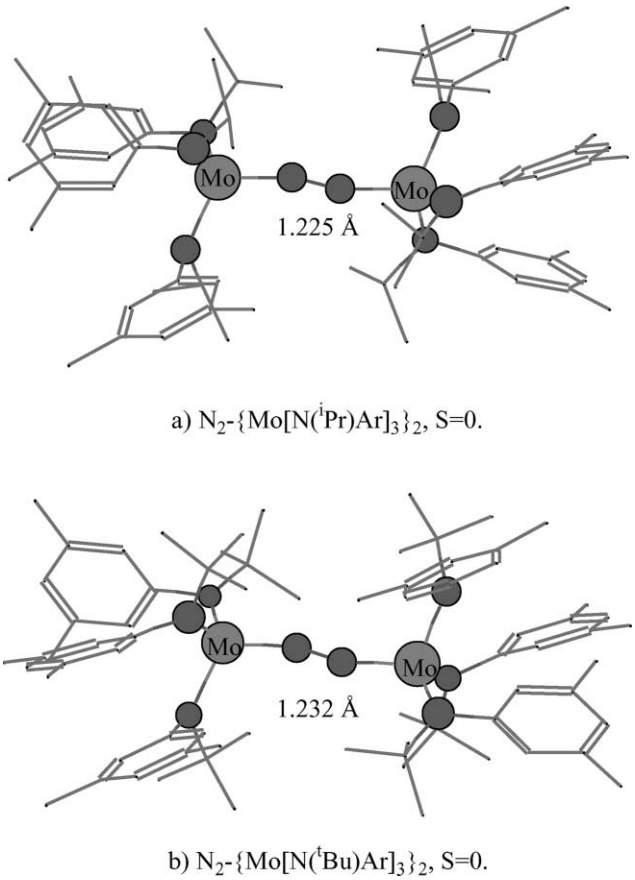

Fig. 5 Optimised structures for singlet N_2-{Mo[N(^{i}Pr)Ar]$_3$}$_2$ and N_2-{Mo[N(^{t}Bu)Ar]$_3$}$_2$ with a single ligand rotated at each metal centre.

Consistent with our calculations for R = ^{i}Pr in the previous section, the lowest energy structure has one of the N(^{i}Pr)Ar ligands bound to Nb rotated. The R = ^{t}Bu ligands, however, maintain a trigonal arrangement around the Mo centre. The structure with ligands rotated at both metal centres lies about 15 kJ mol^{-1} higher in energy. The ligand orientation in the calculated structure is similar to that seen in the crystal structure and the calculated bond lengths and angles are in good agreement with experiment. The average difference between the calculated and experimental bond lengths that have been compared is 0.02 Å. The calculated N–N bond length of 1.226 Å is slightly shorter than the experimentally observed value of 1.235 Å.

It is tempting to explain the structure purely in terms of the relative sizes of the ligands, but the observed ligand orientation cannot be due solely to steric effects. Our calculations in the previous section show that ligand rotation at the Nb centre should still occur if R = ^{t}Bu. Ligand rotation is also favorable for the $Mo^{III}Mo^{III}$ dimer even for the larger N(^{t}Bu)Ar ligands. Calculations on the model system show that ligand rotation is somewhat less favourable for the $Mo^{III}Nb^{III}$ dimer than for the $Mo^{III}Mo^{III}$ dimer, and most of the stabilization due to

Table 3 The effect of ligand rotation on the energy of the experimental $Mo^{III}Nb^{III}$ dimer

Spin state	Symmetry	Ligand rotation[a]	ΔE^b/kJ mol^{-1}	ΔE^c/kJ mol^{-1}	N–N/Å
Doublet	$\approx C_3$	Trigonal	−260.13		1.210
	None	Mo only	[d]		
	None	Nb only	−314.75	−54.62	1.226
	None	Both	−301.09	−40.96	1.211
Quartet	$\approx C_3$	None	−129.04		1.199
	None	Both	−181.85	−52.81	1.205

[a] Ligand rotation refers to the metal center where the rotation, if any, occurs. In all cases ligand rotation is approximately 90°. Ligands trigonal—constrained to a trigonal arrangement. [b] Energy relative to reactants. [c] Energy relative to $\approx C_3$ dimer structure. [d] Not a minimum—optimized to structure with ligands rotated at both metal centers.

ligand rotation is gained when just one ligand is rotated. Ligand rotation is more favourable at the Nb center than Mo and less favorable for R = ^{t}Bu compared to the smaller R = ^{i}Pr. Thus, both the reduced driving force for rotation at the Mo centre relative to Nb, and the increased steric bulk of the ligand are important in determining the overall ligand orientation.

3.3 QM/MM system, L = N(R)Ph

Our calculations on the full ligand system predict a singlet ground state for both L = N(^{t}Bu)Ar and L = N(^{i}Pr)Ar ligands, with a singlet/triplet splitting of 25 kJ mol^{-1}. However, the SQUID magnetometry studies on the related (μ-N_2)-{Mo[N(^{t}Bu)Ph]$_3$}$_2$ dimer give a magnetic moment of $\mu = 2.85\,\mu_B$ consistent with a triplet ground state and the lack of temperature dependence implies that the singlet state is not significantly populated at room temperature. Changing the ligand from N(^{t}Bu)Ar to N(^{t}Bu)Ph is not expected to have a dramatic effect, but in order to check this assumption and to make a direct comparison with experiment, QM/MM calculations were carried out for the L = N(^{t}Bu)Ph system in an analogous manner to those on the L = N(^{t}Bu)Ar system. The results are summarized in Table 4.

The calculated structures for the singlet and triplet states are reasonably similar to those observed for L = N(^{t}Bu)Ar with π stacking clearly evident. The most notable difference between the two systems is the singlet/triplet splitting of only 7 kJ mol^{-1} compared to 25 kJ mol^{-1} for the analogous L = N(^{t}Bu)Ar system. In order to address whether this energy difference is due to electronic or steric effects, single point calculations were performed on the L = N(^{t}Bu)Ph system but using the ligand orientation from the corresponding L = N(^{t}Bu)Ar calculations and *vice versa*.† The energies from these calculations are given in Table 5. Not surprisingly, the single point energies are higher than the energies for the optimized structures, varying from 6 to 42 kJ mol^{-1} higher in energy for the L = N(^{t}Bu)Ph and L = N(^{t}Bu)Ar singlet states, respectively (compare Table 4). The difference is larger for the L = N(^{t}Bu)Ar system since steric crowding is more significant.

Table 5 Energies for single point calculations on the $Mo^{III}Mo^{III}$ dimer L = N(^{t}Bu)Ph at L = N(^{t}Bu)Ar orientations, and *vice versa*

Ligand	Spin state	ΔE^a/kJ mol^{-1}	Splitting/kJ mol^{-1}
N(^{t}Bu)Ph	Singlet	−229.45	
	Triplet	−206.88	22.58
N(^{t}Bu)Ar	Singlet	−195.73	
	Triplet	−190.24	5.49

[a] Energy relative to reactants.

The most interesting point to note is the change in the singlet/triplet splitting which for N(^{t}Bu)Ph has increased from approximately 7 to 23 kJ mol^{-1} (close to that calculated for the Ar system) when the ligand orientation from the optimized L = N(^{t}Bu)Ar system is used. However, when the ligand orientation from L = N(^{t}Bu)Ph is applied to the L = N(^{t}Bu)Ar system, the splitting decreases from 25 to 5.5 kJ mol^{-1}, very close to the optimized value of 7 kJ mol^{-1} found for the Ph system. Both these changes are consistent with the bulky ligands in the L = N(^{t}Bu)Ar system being forced to adopt a less favorable orientation compared to the L = N(^{t}Bu)Ph system due to the greater steric crowding in the former. As a consequence, the singlet/triplet splitting in the L = N(^{t}Bu)Ar system is nearly 20 kJ mol^{-1} greater.

On the basis of these calculations, different ground state properties are predicted for the L = N(^{t}Bu)Ar and L = N(^{t}Bu)Ph systems. The former is calculated to have a singlet ground state and, since the triplet state lies 25 kJ mol^{-1} to higher energy, the complex is expected to be essentially diamagnetic or at best to exhibit weak temperature-dependent paramagnetism. For the Ph system, the calculated singlet–triplet gap is relatively small, so realistically, within the error bounds of the calculations, it is not possible to predict with confidence whether the ground state is a singlet or triplet. Irrespective of the nature of the ground state, temperature dependent paramagnetism is expected given the closeness of the singlet and triplet levels.

† To achieve this the methyl groups were deleted from the Ar ring to convert Ar to Ph and a single point calculation was performed on the modified geometry.

Table 4 Structure and energy of the $Mo^{III}Mo^{III}$ dimer with L = N(^{t}Bu)Ph ligands

Spin state	Symmetry	Ligand rotation[a]	ΔE^b/kJ mol^{-1}	ΔE^c/kJ mol^{-1}	N–N/Å
Singlet	$\approx C_3$	Trigonal			
	None	One only	−212.88		1.229
	None	Both	−235.79		1.236
Triplet	$\approx C_3$	None	−208.67		1.214
	None	One only[d]			
	None	Both	−228.69	−20.01	1.256

[a] Ligand rotation refers to the metal center where the rotation, if any, occurs. In all cases ligand rotation is approximately 90°. [b] Energy relative to reactants. [c] Energy relative to $\approx C_3$ dimer structure. [d] Not a minimum—optimized to structure with ligands rotated at both metal centers.

Although the calculations on the L = N(ᵗBu)Ph system are not entirely consistent with experiment in that the reported magnetic data for this complex indicate little if any population of the higher lying singlet state, they do indicate that the L = N(ᵗBu)Ph and L = N(ᵗBu)Ar systems will have quite different magnetic properties. Consequently, the original assumption that the L = N(ᵗBu)Ar system should behave similarly to the L = N(ᵗBu)Ph system and therefore posses a triplet ground state, is not valid. Indeed, if solid state magnetic measurements on the Ar system are forthcoming, they may well show this complex to posses a singlet ground state.

4 Conclusion

Model calculations using simple NH_2 ligands to replace the bulky N(R)Ar amide groups indicate a strong preference for ligand rotation at both metal centres for the $Mo^{III}Mo^{III}$ and $Mo^{III}Nb^{III}$ intermediate dimers. For the most part, QM/MM calculations on the full systems give similar results to the model calculations implying that the additional stabilization arising from ligand rotation is largely driven by electronic not steric effects.

In the case of the $Mo^{III}Mo^{III}$ dimer, rotation of the N(R)Ar ligands (R = ⁱPr or ᵗBu) is favoured at both metal centres. For the $Mo^{III}Nb^{III}$ dimer, ligand rotation is also favourable but more so at the Nb center than Mo, with the size of the R group having a greater influence on the orientation of the ligands. For R = ⁱPr, rotation is predicted at both Mo and Nb metal centres whereas when R = ᵗBu, the structures involving ligand rotation at both metal centres or rotation at the Nb centre only, are of comparable energy. Calculations on the real $Mo^{III}Nb^{III}$ system $[Ar(^tBu)N]_3Mo$-(μ-N_2)-$Nb[N(^iPr)Ar]_3$ involving both N(ⁱPr)Ar and N(ᵗBu)Ar ligands are in very good agreement with the experimental data in that a spin doublet ground state with ligand rotation only at the Nb centre are predicted.

For the $Mo^{III}Mo^{III}$ system, calculations on the experimental system predict a singlet ground state for the (μ-N_2)-$\{Mo[N(^tBu)Ar]_3\}_2$ dimer with the triplet state lying 25 kJ mol^{-1} higher in energy. This conflicts with the reported magnetic moment for the related (μ-N_2)-$\{Mo[N(^tBu)Ph]_3\}_2$ dimer, which indicates a triplet ground state. Although the magnetic moment was not measured for the experimental complex (μ-N_2)-$\{Mo[N(^tBu)Ar]_3\}_2$, one might have expected the singlet–triplet splitting to be similar for the two systems. However, subsequent QM/MM calculations on the (μ-N_2)-$\{Mo[N(^tBu)Ph]_3\}_2$ dimer have revealed that the singlet–triplet gap is nearly 20 kJ mol^{-1} smaller and, within the error limits of the calculations, it is not possible to determine with confidence whether the singlet or triplet is the ground state. The unexpected but significant difference between these two systems is shown to arise from a more favourable orientation of the bulky amide ligands in the L = N(ᵗBu)Ph system. Since the ground state energetics for these two complexes will give rise to very different magnetic properties, the assumption that (μ-N_2)-$\{Mo[N(^tBu)Ar]_3\}_2$ should posses a triplet ground state analogous to (μ-N_2)-$\{Mo[N(^tBu)Ph]_3\}_2$ cannot be upheld.

Acknowledgements

The authors greatly acknowledge the Australian Research Council for financial support in the form of an Australian Postgraduate Award for G. C. and a Discovery Project Grant for R. S. and B. F. Y. The Australian National University is also acknowledged for funding of this project through the Faculty Research Grant Scheme.

References

1 M. D. Fryzuk and S. A. Johnson, *Coord. Chem. Rev.*, 2000, **200**, 379–409.
2 M. D. Fryzuk, *Chem. Rec.*, 2003, **3**, 2–11.
3 C. E. Laplaza and C. C. Cummins, *Science*, 1995, **268**, 861–863.
4 Q. Cui, D. G. Musaev, M. Svensson, S. Sieber and K. Morokuma, *J. Am. Chem. Soc.*, 1995, **117**, 12366–12367.
5 K. M. Neyman, V. A. Nasluzov, J. Hahn, C. R. Landis and N. Rosch, *Organometallics*, 1997, **16**, 995–1000.
6 G. Christian, J. Driver and R. Stranger, *Faraday Discuss.*, 2003, **124**, 331–341.
7 J. Hahn, C. R. Landis, V. A. Nasluzov, K. M. Neyman and N. Rosch, *Inorg. Chem.*, 1997, **36**, 3947–3951.
8 G. Christian and R. Stranger, *Dalton Trans.*, 2004, **16**, 2492–2495.
9 C. E. Laplaza, M. J. A. Johnson, J. C. Peters, A. L. Odom, E. Kim, C. C. Cummins, G. N. George and I. J. Pickering, *J. Am. Chem. Soc.*, 1996, **118**, 8623.
10 D. J. Mindiola, K. Meyer, J.-P. F. Cherry, T. A. Baker and C. C. Cummins, *Organometallics*, 2000, **19**, 1622–1624.
11 Y. C. Tsai and C. C. Cummins, *Inorg. Chim. Acta*, 2003, **345**, 63–69.
12 G. T. Velde, F. M. Bickelhaupt, E. J. Baerends, C. F. Guerra, S. J. A. Van Gisbergen, J. G. Snijders and T. Ziegler, *J. Comput. Chem*, 2001, **22**, 931–967.
13 C. F. Guerra, J. G. Snijders, G. te Velde and E. J. Baerends, *Theor. Chem. Acc.*, 1998, **99**, 391–403.
14 *ADF2002.03*, SCM, Theoretical Chemistry, Vrije Universiteit, Amsterdam, The Netherlands, 2002, http://www.scm.com.
15 S. H. Vosko, L. Wilk and M. Nusair, *Can. J. Phys.*, 1980, **58**, 1200–1211.
16 A. D. Becke, *Phys. Rev. A*, 1988, **38**, 3098–3100.
17 J. P. Perdew, *Phys. Rev. B*, 1986, **33**, 8822–8824.
18 G. T. Velde and E. J. Baerends, *J. Comput. Phys.*, 1992, **99**, 84–98.
19 L. Versluis and T. Ziegler, *J. Chem. Phys.*, 1988, **88**, 322–328.
20 E. van Lenthe, E. J. Baerends and J. G. Snijders, *J. Chem. Phys.*, 1993, **99**, 4597–4610.
21 E. van Lenthe, E. J. Baerends and J. G. Snijders, *J. Chem. Phys.*, 1994, **101**, 9783–9792.
22 E. van Lenthe, A. Ehlers and E. J. Baerends, *J. Chem. Phys.*, 1999, **110**, 8943–8953.
23 L. Y. Fan and T. Ziegler, *J. Phys. Chem.*, 1992, **96**, 6937–6941.
24 L. Y. Fan and T. Ziegler, *J. Chem. Phys.*, 1992, **96**, 9005–9012.
25 T. K. Woo, L. Cavallo and T. Ziegler, *Theor. Chem. Acc.*, 1998, **100**, 307–313.
26 M. Clark, R. D. Cramer and N. Vanopdenbosch, *J. Comput. Chem*, 1989, **10**, 982–1012.
27 A. K. Rappe, C. J. Casewit, K. S. Colwell, W. A. Goddard and W. M. Skiff, *J. Am. Chem. Soc.*, 1992, **114**, 10024–10035.
28 D. V. Khoroshun, D. G. Musaev and K. Morokuma, *Organometallics*, 1999, **18**, 5653–5660.
29 T. Ziegler, A. Rauk and E. J. Baerends, *Theor. Chem. Acc.*, 1977, **43**, 261–271.
30 R. Stranger, J. E. McGrady and T. Lovell, *Inorg. Chem.*, 1998, **37**, 6795–6806.